RESEARCH ARTICLE

Editor's Choice

ADVANCED MATERIALS TECHNOLOGIES

www.advmattechnol.de

A Coplanar Edible Rechargeable Battery with Enhanced Capacity

*Valerio Galli, Valerio F. Annese, Giulia Coco, Pietro Cataldi, Vincenzo Scribano, Ivan K. Ilic, Athanassia Athanassiou, and Mario Caironi**

Edible rechargeable batteries represent a novel opportunity for energy storage, which currently involves the use of toxic materials. Being entirely made of food-derived materials and additives, such batteries open the way to electronic systems characterized by unprecedented features. Their sustainability and safety can be crucial for replacing traditional batteries in low-power applications, like agrifood and medicine, reducing environmental impact and health hazards. Yet, limitations in capacity and architecture, and concerns about stability at elevated temperature, humidity, and prolonged storage time, severely limit their current application potential. Here, a new coplanar architecture of a riboflavin-quercetin edible battery with increased capacity, reaching 20 µAh, and operational stability of two weeks is presented. The battery is tested in diverse environmental conditions to assess its possible implementation in different scenarios, showing stable performance between 0 and 37 °C. As a proof-of-concept application, the coplanar architecture is exploited to develop a 3-cell battery with a voltage of ≈2 V and demonstrate the possibility of powering a commercial Internet of Things (IoT) module. The new design and data herein presented represent significant steps toward widening the opportunities offered by edible batteries and their implementation in low-power electronics.

1. Introduction

Nowadays, batteries are ubiquitous in our society and significantly affect our lives. From electric vehicles to portable electronic devices, the development and spread of rechargeable batteries have changed and improved our quality of life. They are also one of the key aspects of the green energy revolution, allowing the storage of energy produced through renewable sources. Considering only lithium-ion batteries, the global demand has reached 700 GWh in 2022 and is expected to reach 4.7 TWh in 2030.[1] However, both non-rechargeable and rechargeable batteries represent a serious environmental threat along the whole lifecycle. The battery industry employs hazardous and toxic materials and highly environmentally impacting processes from manufacturing to disposal. In particular, the battery end-of-life is often neglected, and standardized recycling processes are still complex, which may lead to landfill disposal or incineration.[2,3] These disposal routes might contaminate soil, air, and water, severely threatening wildlife and humans. Once dispersed in the environment, batteries can release different toxic chemical compounds like gasses (HF, HCl, vapor of organic solvents), liquids (organic electrolytes, ionic liquids), and heavy metals (Cr, Co, Cu, Pb, Ni, Mn, Hg) that might contaminate groundwater, spreading the pollutants far from the landfill site.[2,3] Furthermore, these released compounds may poison wildlife and humans, with lethal consequences after long exposure.[2,3]

These safety and pollution concerns are particularly relevant in healthcare and environmental monitoring applications. Large-scale data collection through low-power, portable, disposable, and low-cost electronics would improve human life and support nature preservation. Nonetheless, such innovation can be sustained only by enabling the use of distributed and pervasive electronics without contributing to electronic waste accumulation and related environmental pollution. Hence, the quest for more sustainable and environmentally friendly energy sources.

The development of biodegradable batteries[4–9] can offer a partial solution, although environmental pollution and safety risks

V. Galli, V. F. Annese, G. Coco, I. K. Ilic, M. Caironi
Center for Nano Science and Technology
Istituto Italiano di Tecnologia
Via Rubattino 81, Milan 20134, Italy
E-mail: mario.caironi@iit.it

V. Galli, G. Coco
Department of Physics
Politecnico di Milano
Piazza Leonardo da Vinci, 32, Milan 20133, Italy

P. Cataldi, V. Scribano, A. Athanassiou
Smart Materials
Istituto Italiano di Tecnologia
Via Morego 30, Genova 16163, Italy

The ORCID identification number(s) for the author(s) of this article can be found under https://doi.org/10.1002/admt.202400715

DOI: 10.1002/admt.202400715

are not completely eliminated since some critical aspects related to biodegradability are not always considered. Indeed, the redox-active materials exploited in biodegradable batteries are organic molecules and metal oxides, which are often toxic if ingested by animals or humans.[4–9] Moreover, biodegradable polymers can be fragmented and, in a similar way to conventional polymers, produce microplastics and nanoplastics, especially in the aqueous environment.[10,11] Besides being a threat to living organisms, microplastics can also be a vector for chemical pollutants and microorganisms, due to their size and chemistry.[10,11] These are significant limits to the implementation of biodegradable batteries in healthcare, especially for ingestible systems, and in agrifood applications. In healthcare, ingestible non-edible electronics is becoming attractive for replacing invasive diagnostics techniques like endoscopy and colonoscopy. Yet, hospitalization is still required due to the retention risk and possible toxic chemical leaks.[12,13] In the agrifood sector, the deployment of sensors in agricultural fields will significantly improve local parameter monitoring and data acquisition, optimizing the management strategy and the use of agrochemicals.[14–17] However, the spread of a large number of battery-powered sensors in agricultural fields can lead to environmental pollution and wildlife poisoning if batteries are dispersed or damaged.

In these application scenarios, edible materials become particularly interesting for developing completely safe electronics.[18–21] Several materials and devices have been demonstrated in recent years, like resistors,[22] transistors,[23,24] sensors,[25–29] actuators,[25,30–32] and power sources,[33–38] as well as communication strategies.[39] Such demonstrations are the starting point to create a safe-to-ingest technology that can replace standard electronics in both healthcare and agrifood scenarios: edible systems can replace ingestible electronics for gastrointestinal (GI) tract monitoring, eliminating any retention risk; edible smart tags can be directly applied to food for monitoring and avoiding spoilage or counterfeiting.[18]

Ilic et al.[40] recently developed the first edible rechargeable battery, entirely composed of food materials, which exploits a redox reaction between two molecules commonly found in food, riboflavin and quercetin. This battery has an operating voltage of ≈0.65 V and a capacity of ≈10 µAh, sustaining a current of 48 µA for 12 min.[40] Besides its use in edible electronics, it has the potential to replace traditional batteries in low-power applications, as recently shown through a preliminary interconnection with passive sensors for environmental monitoring.[41,42] However, the capacity of this prototype is limited, the electrode architecture is not optimized for interconnection with other components, and its stability in time and different environmental conditions, relevant for future application scenarios, has not been assessed yet.

Here we propose a coplanar edible rechargeable battery with a twofold capacity increase with respect to the first literature report and proven operational stability in different environmental conditions. The new coplanar electrode configuration, which does not limit battery performance, favors the interconnection with other electronic components and multiple battery connections. The improved battery performance, reaching a capacity of ≈20 µAh, was achieved by adopting a higher electrode mass loading, without overcoming the acceptable daily intake (ADI) values of the edible materials used. The edible battery retains its capacity over two weeks of storage at room temperature, whereas freezing hampers battery self-discharge. Powering of a commercial Bluetooth-based Internet of Things (IoT) module is achieved with two 3-cell batteries, providing a proof-of-concept demonstration of future environmental monitoring applications. Our results indicate a feasible path along the development of edible batteries as critical components in sustainable IoT nodes as well as power supplies in future edible electronic systems for pharmaceutical and food monitoring applications.

2. Results and Discussion

To realize the edible rechargeable battery, we made use of food-grade materials only, that can be eaten in large amounts without any safety risk.[40] The redox chemistry of the battery corresponds to the one recently reported by Ilic et al.[40] and is based on two small redox-active molecules, riboflavin and quercetin, used for the anode and the cathode, respectively. Riboflavin (RF), or vitamin B_2, is a natural redox cofactor and is used as a food coloring agent (E 101) and vitamin supplement. Quercetin (Q) is a flavonoid found in vegetables and seeds, sold also as a dietary supplement. Due to their poor electrical conductivity, the two redox-active molecules were mixed with activated carbon (AC, E 153), a safe-to-eat electronic conductor, to allow electron transport. These composites were used to prepare the redox-active inks, using ethyl cellulose (EC, E 462) dissolved in ethanol as the binder. The inks were then deposited onto edible current collectors to form the electrodes. The current collectors were fabricated by laminating edible gold (E 175) leaves onto EC films. However, the gold-EC films have just one conductive side due to their fabrication process and this aspect complicated the interconnection of the first example of an edible battery[40] with electronic components. To overcome such limitation, we adopted an electrode coplanar configuration, as illustrated in the scheme of **Figure 1a**, improving multiple battery connections (series and parallel) and compatibility with other components.[23,24,29] The battery was completed by placing Nori, soaked in a 1 M aqueous solution of $NaHSO_4$ (E 514ii), used as the electrolyte, on top of the electrodes, and encapsulating the device with beeswax (E 901). A photograph of the fabricated coplanar battery is shown in Figure 1c. All the materials used to fabricate the battery are approved as edible by the European Food Safety Authority (EFSA) and their quantities per single device do not exceed the ADI values (**Table 1**).

The new electrode coplanar configuration was tested with a starting composite mass loading of 1.5 mg cm^{-2} to compare its performance with the previously reported edible battery stacked architecture, which had such composite mass loading.[40] The direct comparison between the two architectures is crucial to evaluate whether the planar ionic transport between the electrodes, over a cm range distance, introduced with the coplanar configuration, could pose limits to the battery performance as obtained with a vertical ionic transport, over a mm range distance.[40] The battery capacity was evaluated through galvanostatic charging-discharging measurements between 0.6 and 0.8 V at different currents. This voltage window is related to the redox plateau, i.e. the voltage range where the device properly works as a secondary battery.[40] The battery is not cycled at higher or lower voltages to not damage it irreversibly. This is a common practice in

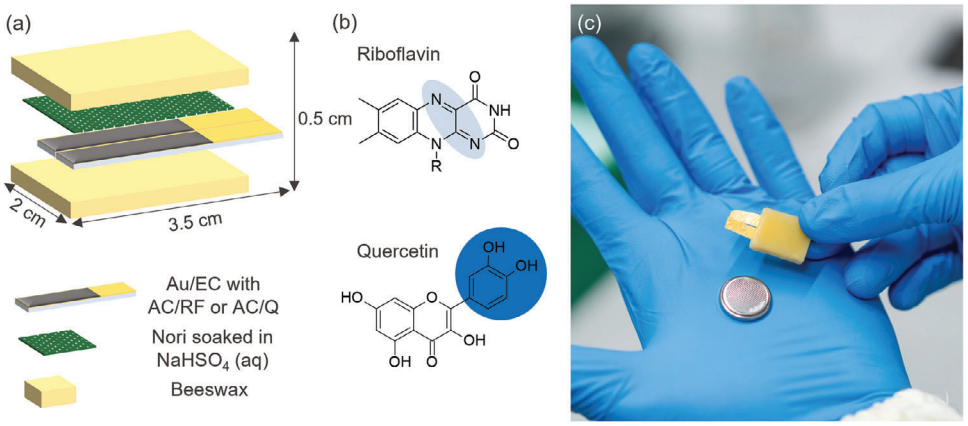

Figure 1. Edible rechargeable coplanar battery. a) Coplanar battery design and edible materials used. b) Small redox-active molecules, riboflavin and quercetin, in their natural discharged state. c) Dimension comparison with a CR2032 button cell.

commercial batteries to prevent their failure. The capacity values of coplanar batteries (≈10 µAh), calculated from the curves, were consistent with those of stacked batteries obtained in previous works[40,41] (Figure S1, Supporting Information), confirming no performance limitation owing to the new coplanar design and the planar ionic transport. The possibility to refine the battery design without capacity losses is a crucial aspect for interconnection with other components, optimizing connections depending on the final application.

Table 1. Edible rechargeable battery ingredients. The amount of each edible material in one battery is compared to edibility data from EFSA (NOAEL: no-observed-adverse-effect level).

Ingredients	E number	One battery contains	Edibility per day	refs.
Quercetin	Food ingredient	0.54 mg	Consumption estimate: 25–50 mg	[43]
Riboflavin	E 101	0.54 mg	Average requirement: 1.6 mg	[44]
Activated carbon	E 153	4.32 mg	Daily recommended serving: hundreds of milligrams	[45]
Gold	E 175	1.4 mg	No risk assessment	[46]
Ethyl cellulose	E 462	36 mg	Indicative total exposure: 660–900 mg per kg of body weight	[47]
Sodium hydrogen sulfate	E 514(ii)	35 mg	Laxative effect: doses greater than 300 mg per kg of body weight	[48]
Nori	Food	25 mg	N/A (food)	–
Water	Food	290 mg	N/A (food)	–
Beeswax	E 901	1.5 g	NOAEL: 1.1 g per kg of body weight	[49]

To improve the battery capacity, limited by the low conductivity of activated carbon and the lack of more performing edible conductive fillers, the electrode mass loading was then increased to 3 mg cm^{-2}. The galvanostatic charging-discharging capacity of the battery with doubled mass loading results correspondingly doubled at each tested current, reaching a maximum value of ≈20 µAh at 100 µA (**Figure 2a**). It is noteworthy that the increased capacity has been obtained without increasing the active area and current collector dimensions, and without overcoming the materials ADI (Table 1). Moreover, the galvanostatic data demonstrate good capacity retention in the range of 100–10 µA, allowing a quick battery charging with a high current (100 µA) and a slower discharging with lower currents (10 µA, Figure S2, Supporting Information). Our edible batteries can supply a current of 100 µA for 12 min, 50 µA for 20 min, and 10 µA for more than one hour, as it can be observed from the discharging curves in Figure 2b. Discharge times were also evaluated using commercial resistors, to determine the battery behavior when connected to an external resistive load. The curves in Figure 2c,d show a battery discharge time of ≈20 min when connected to a 12 kΩ load and >2 h when connected to a 120 kΩ load. Given these results, the new mass loading was adopted in all the subsequent measurements.

Stability over time and at different temperature and humidity values is often a limiting aspect in aqueous batteries, which are subject to water evaporation and variations in electrolyte ionic conductivity, leading to performance degradation over time.[50] For this reason, the first stability assessment on edible batteries was performed, testing them under different conditions. First, batteries were cycled over three consecutive days, through 20 charging-discharging cycles per day, to study their operational stability over time. Results in **Figure 3a** show stable capacity values over three days at room temperature and humidity (20 °C, 35% RH) and a coulombic efficiency that increases over time and reaches 95% at the end of the test. We speculate that the increase can be caused by a molecular rearrangement inside the composites during battery cycling. A longer-term stability

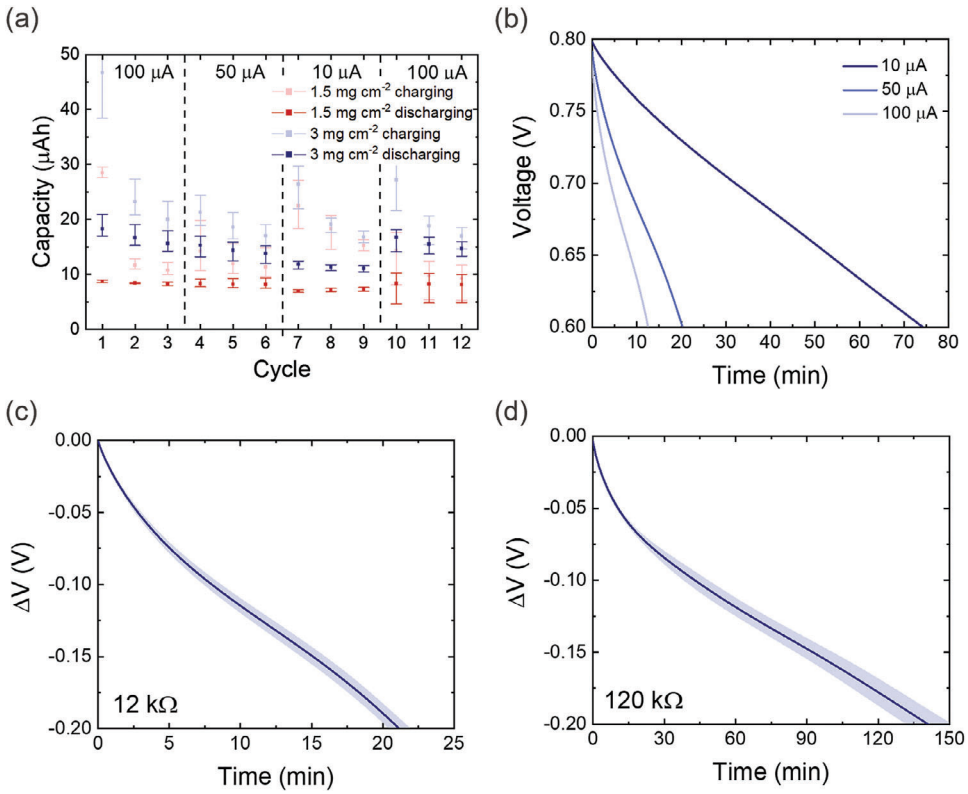

Figure 2. Coplanar battery testing. a) Galvanostatic charging-discharging capacities of three coplanar batteries at different currents, comparing the 1.5 mg cm^{-2} mass loading (red) with the 3 mg cm^{-2} one (blue). b) Corresponding charging–discharging curves from one of the batteries (3 mg cm^{-2} mass loading). c) Average discharging curves and standard deviation calculated over three batteries when connected to 12 kΩ and d) 120 kΩ loads (3 mg cm^{-2} mass loading).

test was done by cycling batteries over a month, performing a charging-discharging cycle each day for the first week, and then cycling the batteries on the 10th, 14th, 21st, and 28th days. During such month, batteries were stored at room temperature and humidity (20 °C, 35% RH). Capacity values reported in Figure 3b show excellent operational stability over two weeks. In the third and fourth weeks, a progressive capacity decrease can be observed, probably associated with redox molecule degradation or leakages.

The battery fabrication process, which is currently mainly manual, leads to unavoidable defects and imperfections, which can favor oxygen permeation and consequently limit battery performance, affecting in particular its self-discharge. Battery self-discharge was evaluated through open circuit (OC) measurements and curves in Figure S3 (Supporting Information) show an average self-discharge time of 24 h. The presence of oxygen can be a cause; however, further investigations are required to properly identify the self-discharge mechanism.[51] This limitation can be easily overcome by storing charged batteries in a commercial freezer at −21 °C. The battery OC voltages were continuously measured with a sampling rate of 5 min while frozen and data in Figure 3c show very good charge retention, with a maximum decrease of ≈4% after 84 h. This simple storage method, commonly used for drugs and food, allows the use of edible batteries days after their fabrication and charging without any significant charge loss.

The possibility of employing the battery in different scenarios, like GI tract monitoring or agrifood, was preliminary assessed by testing the batteries in different environmental conditions, varying temperature and RH. Galvanostatic charging–discharging measurements were performed in an environmental chamber, starting from room conditions (20 °C, 65% RH), and then simulating storage conditions in a fridge (5 °C, 65% RH), and human GI tract (37 °C, 90% RH). The batteries were also cycled in low temperature-high RH (0 °C, 85% RH) and high temperature-low RH (50 °C, 25% RH) conditions. The complete time-temperature/RH testing plot is reported in Figure S4 (Supporting Information). Batteries showed comparable and stable capacity values in all the tested conditions, with a decrease in performance at high temperatures (average capacity equal to 16.8 µAh at 20 °C, 13.2 µAh at 37 °C, and 10 µAh at 50 °C), and a recovery of their original capacity when cycled again at room conditions (Figure 3d). These results suggest a maximum battery working temperature of 50 °C to avoid irreversible damage. Indeed, higher temperatures would lead to beeswax melting (≈64 °C)[52] and could deteriorate the other edible materials used. This good operational stability over time and in different environmental conditions can be ascribed to the beeswax encapsulation, which limits oxygen permeation inside the battery and avoids water-electrolyte evaporation. Beeswax also offers good antimicrobial properties, an important aspect for food contact applications.[52] The concentrated acidic electrolyte, which maintains good ionic

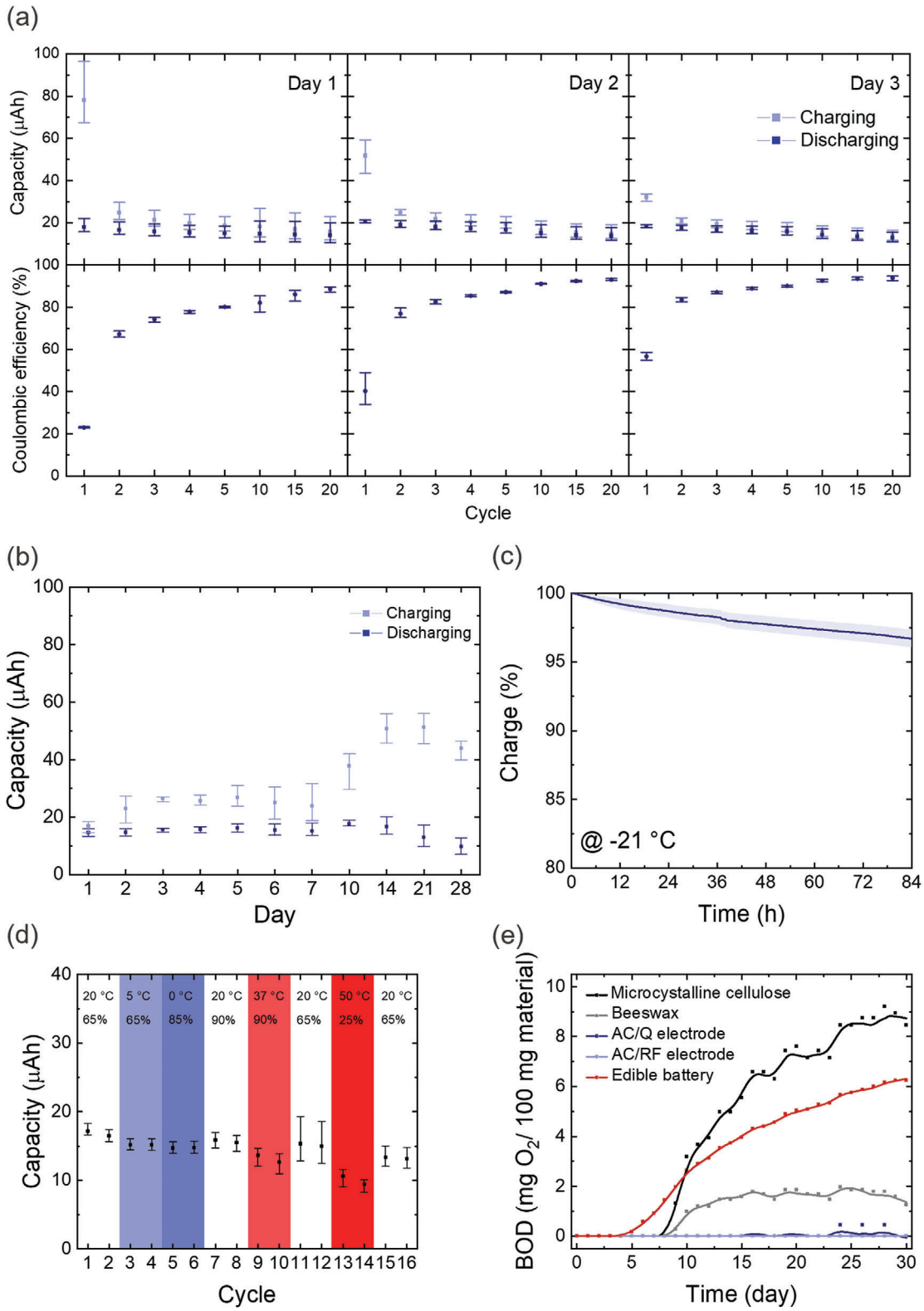

Figure 3. Stability and environmental tests. a) Galvanostatic charging–discharging capacities of three coplanar batteries at 100 μA over three consecutive days. The corresponding coulombic efficiency is also reported. b) Galvanostatic charging-discharging capacities at 100 μA over a month. Three batteries were cycled in the first seven days and then on the 10th, 14th, 21st, and 28th days. c) Average charge retention and standard deviation calculated over three edible batteries stored in a freezer at −21 °C. d) Galvanostatic discharging capacities at 100 μA of three batteries, acquired varying temperature and RH in an environmental chamber. Temperature and RH tested values are reported in the plot. e) Biochemical Oxygen Demand (BOD_{30}) of the edible battery and components. Microcrystalline cellulose and pristine beeswax are used as a reference. The anode and the cathode BOD_{30} are also reported.

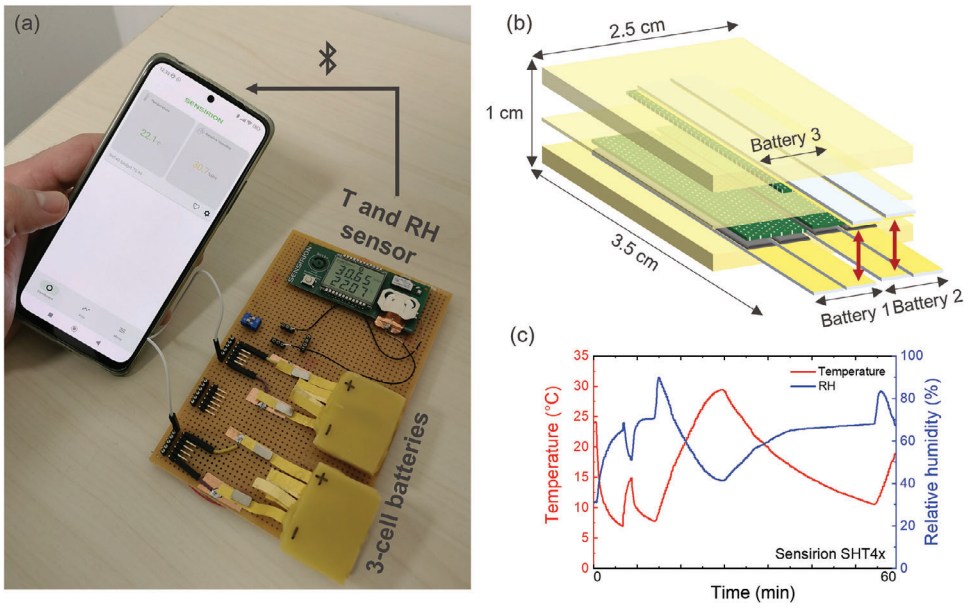

Figure 4. IoT module powered by 3-cell edible batteries. a) Smart Gadget SHT4x module powered by two 3-cell edible batteries connected in series transmitting temperature and RH data in real-time via Bluetooth to a smartphone. b) 3-cell edible battery design. c) Data from a Smart Gadget SHT4x module powered by two 3-cell edible batteries connected in series tested in an environmental chamber, changing temperature and RH over an hour.

conductivity below 4 °C, also plays an important role in stabilizing battery capacity at low temperatures. These effects are confirmed by electrochemical impedance spectroscopy (EIS) measurements at 20 and 0 °C (Figure S5, Supporting Information).

The integration of sustainable and completely biodegradable batteries in low-power sensing nodes may be beneficial to the large-scale spread of environmental monitoring devices, avoiding their recollection after use. For this reason, edible battery biodegradability was preliminarily evaluated in seawater,[53] where commonly used biodegradable polymers (polyhydroxybutyrate, polycaprolactone, polylactic acid) show, on average, lower degradation than in soil.[54] The test followed the test method ISO 23977-2:2020, which standardizes how to measure the biochemical oxygen demand in seawater over 30 days (BOD_{30}), corresponding to the amount of aerobic bacteria oxygen consumption in the decomposition process (Figure 3e). Battery electrodes, pristine as-received beeswax, and microcrystalline cellulose used as a positive reference due to its established degradability in seawater,[55] were also tested. During the 30 days, the battery electrodes did not show a detectable BOD_{30} signal due to the low degradation rate of EC, the primary component of the electrodes.[56] Pristine beeswax degraded over time, with a start in the degradation after seven days, reaching ≈1.5 mg O_2/100 mg BOD_{30}. Degradation was also observed in batteries, previously cut along the cross section to expose the electrodes to seawater. Interestingly, their biodegradability was higher compared to the pristine beeswax, reaching up to 6 mg O_2 consumed per same amount of material, and the degradation process started only after four days. This behavior may be due to the presence of Nori, which could have favored bacterial activity, and/or to the difference in beeswax crystallinity between the pristine one used as a control and the one treated (i.e., melted and solidified) for encapsulation. Indeed, a fast cooling rate may induce a lower crystallinity, resulting in quicker and higher biodegradation.[10,57,58]

The stability, sustainability, and safety of the battery offer new opportunities in low-power electronics, especially in healthcare, since the operating voltage (≈0.65 V) is perfectly safe for applications inside the human body. However, this voltage might represent a limit for the interconnection of the edible battery with traditional electronics in agrifood applications. As such, to propose a proof-of-concept demonstration of future potential applications, a 3-cell battery was developed by connecting in series three coplanar batteries by adjacent electrode overlap and integrating them into a single beeswax case (**Figure 4**). In the 3-cell battery, two single-cell batteries are placed adjacently on the same plane with the electrodes facing upwards. A third single-cell battery is stacked on top, with the electrodes facing downwards to facilitate the series connection. Overlapping electrodes were electrically interconnected (Figure 4b; Figure S6, Supporting Information). 3-cell battery dimensions (3.5 cm x 2.5 cm x 1 cm) are just slightly larger than those of a single coplanar battery (Figure S7a, Supporting Information). This battery has an operating voltage of ≈2 V and retains the same capacity of a single cell, showing a discharge time of ≈10 min with a current of 100 µA (Figure S7b, Supporting Information).

We finally prove the compatibility of the edible batteries with low-power traditional electronics by connecting two 3-cell batteries in series to power a commercial IoT module (Sensirion Smart Gadget SHT4x) that can monitor environmental temperature and RH, and transmit real-time data via Bluetooth. The batteries were able to supply an OC voltage higher than 4 V, enough to switch on the LCD screen and power the IoT module, acquiring temperature and RH data in real-time every two seconds (Figure 4a; Video S1, Supporting Information). To simulate a real application, the IoT module, powered by the edible batteries, was tested in an environmental chamber. Temperature and RH were externally controlled and monitored through the IoT module for an hour. Real-time data were transmitted via Bluetooth to a smartphone

(Figure 4c), in perfect agreement with data from the environmental chamber sensors (Figure S8a, Supporting Information). The maximum run time of the edible batteries was also tested, reaching 90 min while powering the IoT module at room temperature (Figure S8b, Supporting Information).

3. Conclusion

In this work, we presented a coplanar edible rechargeable battery with enhanced capacity and operational stability in different environmental conditions. The battery benefits from a new coplanar electrode configuration, which, without limiting the battery performance, allows easier multiple battery connections and better interconnection with electronic components.

Through the optimization of the electrode mass loading, we were able to increase the battery capacity up to ≈20 µAh, without increasing the electrode dimensions and without overcoming the ADI of the edible materials used. Stability tests over time, at variable temperature and humidity levels, showed promising results for the use of our edible battery in place of traditional batteries in low-power applications where accidental toxic chemical leakage and battery dispersion in the environment should be avoided. The capacity remains stable for two weeks when batteries are stored at room temperature and humidity. Environmental tests showed that edible batteries can work in a temperature range between 0 and 37 °C with different RH values and can be easily stored in a freezer, retaining more than 96% of their charge after 84 h. A first biodegradability assessment of edible batteries was performed, reaching up to 6 mg O_2 consumed per 100 mg of material within 30 days. The new architecture offers the possibility to connect 3-battery cells in series and integrate them into a single multi-cell battery with a voltage of ≈2 V. A proof-of-concept application in agrifood sensor networks, testing the possible replacement of traditional batteries in low-power devices for sensing and monitoring, was also demonstrated, powering a commercial IoT module with two 3-cell batteries connected in series. The low-power module monitored environmental temperature and RH for 90 min, transmitting real-time data via Bluetooth to a smartphone.

Besides applications in environmental monitoring, the edibility of our battery offers the possibility to integrate electronic sensors directly on food, without any contamination risk deriving from traditional batteries leakages. The complete edibility of our battery is also an innovative solution for powering ingestible electronics, reducing the risk of toxic chemical leaks in case of breakage inside the GI tract. Further capacity increase and miniaturization of the edible battery, together with the development of fully edible electronics, will open the way to completely new agrifood and GI tract monitoring devices.

4. Experimental Section

Riboflavin (≥98%), ethyl cellulose (48.0–49.5% (w/w) ethoxyl basis), sodium hydroxide, and cellulose were purchased from Sigma Aldrich. Quercetin dihydrate (97%) and sodium bisulfate monohydrate ($NaHSO_4$) (≥99.0%) were purchased from Acros Organics. Absolute ethanol was purchased from Sigma Aldrich and Carlo Erba. Beeswax was purchased from Bienenbiya. Activated carbon was purchased from Nature's Way under the name Charcoal, Activated (LOT: 21043A). 23 Karat gold leaves were purchased from Gold Chef – Giusto Manetti Battiloro S.p.A. Sushi Nori was purchased from Alimenta Srl. 12 and 120 kΩ resistors were purchased from Tyco Electronics. Smart Gadget SHT4x Sensirion module was purchased from RS Components S.r.l.

Activated Carbon-Small Molecule (RF/Q) Composites: Small molecules (RF or Q) (0.2 g) and activated carbon (0.8 g) were dispersed together in a mixture of water (25 mL) and ethanol (25 mL). The dispersions were stirred at room temperature for 20 h, and afterward, the solvent was removed under reduced pressure at 60 °C. The formed composites were vacuum-dried for 24 h.

Gold-Laminated Ethyl Cellulose Films: Ethyl cellulose was dissolved in ethanol with a concentration of 20 g L^{-1}. A 30 mL of solution was poured into a Petri dish (9.5 cm in diameter) and oven-evaporated at 60 °C for 17 h. The formed ethyl cellulose films were removed from the Petri dish, with the aid of water, with a razor. The ethyl cellulose film's flat bottom was dampened with ethanol and placed on an edible gold foil to laminate gold onto it. The films with gold were dried in air for a few hours with a weight placed on the top (e.g., a smaller Petri dish). Afterward, the films were hot pressed at 5 MPa and 90 °C for 2 min. The current collectors were prepared by cutting the film in stripes that were 5 mm wide.

Inks Preparation: The desired composite (90 mg) was dispersed in a 15 g L^{-1} solution of ethyl cellulose in ethanol (0.67 mL). The inks were stirred overnight before using them and they were not used for more than 3 days after preparation.

Edible Battery Fabrication: Anode and cathode electrodes were prepared by coating through pipette drop-casting 1 cm^2 of the gold laminated EC current collectors with RF ink (20 µL) and Q ink (20 µL), respectively, and dried under nitrogen flux for 1 h. Beeswax was melted at 100 °C and then poured into a silicon mold to prepare beeswax blocks. The two electrodes were placed one next to the other, with a gap smaller than 1 mm, onto a beeswax block and covered with Nori previously soaked in the 1 M $NaHSO_4$ water electrolyte, to remove as much as possible unwanted salts contained in commercial Nori. The electrolyte was deoxygenated with nitrogen flux before using it. A second beeswax block was placed on top to close the battery and the edges were sealed using molten beeswax. All these fabrication steps were done under nitrogen flux. The approximate dimensions of the edible battery were 3.5 cm × 2 cm x 0.5 cm.

3-Cell Edible Battery Fabrication: Battery electrodes were fabricated as previously described. Two single-cell batteries (electrodes and soaked Nori) were placed adjacently on a beeswax block with the electrodes facing upwards and isolated with smaller beeswax blocks. A third cell was placed on top, with the electrode conductive side facing downwards, to connect the tree cells in series (Figure 4b). Overlapping electrodes were electrically connected with silver paint. A final beeswax block was used to encapsulate the battery (Figure S6, Supporting Information). The approximate dimensions of the 3-cell edible battery were 3.5 cm x 2.5 cm x 1 cm.

Battery Testing: All measurements were performed using MultiPalmSens4 potentiostat. The battery cathode was connected as the working electrode, while the battery anode was the counter/reference electrode. All the tests were simultaneously performed on three batteries.

Galvanostatic charging–discharging measurements were performed at 100, 50, 10, and again 100 µA and cycled for 3 cycles at each charging rate. The charging–discharging curves in Figure 2b are the 1st, 4th, and 7th cycles, respectively.

Discharging curves were also acquired by connecting the batteries to 12 and 120 kΩ resistors and measuring the battery voltage over time.

Stability and coulombic efficiency tests were performed at 100 µA, cycling the batteries for 20 cycles per day for 3 consecutive days. Month-stability test was performed at 100 µA, cycling the batteries for one cycle for seven consecutive days and on the 10th, 14th, 21st, and 28th days. During the test, batteries were stored at room temperature and RH (20 °C, 35%).

Self-discharge curves were acquired through OC measurements with a sampling rate of 5 min over 24 h at room temperature after charging the batteries at 100 µA. The same test was then repeated storing the batteries in a Liebherr MediLine freezer at −21 °C and measuring the OC voltage over 84 h.

Environmental stability tests were performed in a Memmert HPP110ecoplus constant climate chamber, varying temperature, and RH. Batteries were cycled at 100 μA for 2 cycles at each different environmental condition. The test was performed over 3 consecutive days.

Battery capacities were calculated from galvanostatic charging–discharging measurements as:

$$c = I \times t/3600 \quad (1)$$

where c is the battery capacity (μAh), I is the charging/discharging current (μA), and t is the charging/discharging time (s). Capacities were calculated in the voltage window between 0.6 and 0.8 V for single coplanar batteries and between 1.8 and 2.4 V for 3-cell batteries. The first charging capacity reported has always a significantly higher value since it is calculated from 0 V (completely discharged battery).

Coulombic efficiencies (%) were calculated as the ratio between discharging and charging capacities.

All the capacities were calculated from minimum triplicate measurements (calculated in MS Excel), and the average value with maximum and minimum values are shown.

Electrochemical impedance spectroscopy (EIS) of the battery electrolyte was measured using Nori soaked in 1 M $NaHSO_4$ water electrolyte and two gold-laminated EC electrodes, encapsulating everything in beeswax. The impedance was measured by applying a sinusoidal stimulus of 100 mV within a frequency range of 10 mHz–1 MHz. Data were acquired at 20 and 0 °C in a Memmert HPP110ecoplus constant climate chamber.

Smart Gadget SHT4x Sensirion module was powered by two 3-cell edible batteries connected in series. Temperature and RH data were acquired in real time through Sensirion MyAmbience App, connected to the IoT module via Bluetooth connection.

Biochemical Oxygen Demand (BOD) Test Details: The BOD instrumentation (OxiTop OC 100) was used to test the biodegradability of edible batteries in marine environments. The test followed the standard ISO 23977-2:2020. Microcrystalline cellulose and pristine beeswax were used as a reference. The different samples were cut into various shapes, ≈1 cm^2 in size, with a weight ranging from 30 to 300 mg, and inserted in 432 mL of seawater collected from Porto Antico, Genoa (Italy). The tested samples were the battery, with two cuts along the cross section to expose the electrodes to seawater, the anode, and the cathode.

The experiment was conducted by adding the testing materials and seawater into autoclaved 510 mL amber glass bottles and subsequently sealed with the OxiTop OC 100 measuring heads. A stirring magnet was added to ensure constant movement inside the bottle. Sodium hydroxide was added as a CO_2 scavenger to sequester carbon dioxide produced from biodegradation. The oxygen consumption in the free volume was measured as a function of decreased pressure. The raw oxygen consumption data (mg O_2 L^{-1}) were corrected by subtracting the blank values from reference seawater oxygen consumption. The data were then divided by the specific mass samples and normalized to 100 mg of material (mg O_2 per 100 mg material). The data were plotted as the function of mg O_2 per 100 mg of material in one L of seawater over time. LOWESS (Locally Weighted Scatterplot Smoothing) was applied using the default Origin function to smooth out the curves. Measurement was maximized over 30 days (360 measurements per sample). In Figure 3e, one dot per day is a representative trend of degradation. Degradation lines are derived from the smoothing of the dots using the LOWESS function.

Supporting Information

Supporting Information is available from the Wiley Online Library or from the author.

Acknowledgements

V.G., V.F.A., G.C., and M.C. acknowledge the support of the European Union's Horizon 2020 research and innovation program under Grant Agreement #964596 "ROBOFOOD". I.I. and M.C. acknowledge the support of the European Research Council (ERC) under the European Union's Horizon 2020 research and innovation program "ELFO" Grant Agreement #864299. V.F.A. acknowledges funding from the Marie Skłodowska-Curie actions (project name: "EDISENS", Grant Agreement #101105418) under the European Union's Horizon 2020 research and innovation program. P.C. acknowledges funding from the Marie Skłodowska-Curie actions (project name: "BioConTact", Grant Agreement #101022279) under the European Union's Horizon 2020 research and innovation program. The authors acknowledge Camilla Rinaldi for her help with the BOD setup. This work was part of the IIT Flagship project on Technologies for Sustainability.

Open access publishing facilitated by Istituto Italiano di Tecnologia, as part of the Wiley - CRUI-CARE agreement.

Conflict of Interest

The authors declare no conflict of interest.

Data Availability Statement

The data that support the findings of this study are available from the corresponding author upon reasonable request.

Keywords

biodegradable batteries, edible batteries, edible electronics, energy storage, sustainable electronics

Received: May 4, 2024
Revised: July 4, 2024
Published online:

[1] J. Fleischmann, M. Hanicke, E. Horetsky, D. Ibrahim, S. Jautelat, M. Linder, P. Schaufuss, L. Torscht, A. van de Rijt, *McKinsey & Company* **2023**, 2.
[2] A. R. Dehghani-Sanij, E. Tharumalingam, M. B. Dusseault, R. Fraser, *Renewable Sustainable Energy Rev.* **2019**, *104*, 192.
[3] W. Mrozik, M. A. Rajaeifar, O. Heidrich, P. Christensen, *Energy Environ. Sci.* **2021**, *14*, 6099.
[4] M. Karami-Mosammam, D. Danninger, D. Schiller, M. Kaltenbrunner, *Adv. Mater.* **2022**, *34*, 202204457.
[5] X. Huang, D. Wang, Z. Yuan, W. Xie, Y. Wu, R. Li, Y. Zhao, D. Luo, L. Cen, B. Chen, H. Wu, H. Xu, X. Sheng, M. Zhang, L. Zhao, L. Yin, *Small* **2018**, *14*, 1800994.
[6] N. Delaporte, G. Lajoie, S. Collin-Martin, K. Zaghib, *Sci. Rep.* **2020**, *10*, 3812.
[7] M. Navarro-Segarra, C. Tortosa, C. Ruiz-Díez, D. Desmaële, T. Gea, R. Barrena, N. Sabaté, J. P. Esquivel, *Energy Environ. Sci.* **2022**, *15*, 2900.
[8] M. H. Lee, J. Lee, S. K. Jung, D. Kang, M. S. Park, G. D. Cha, K. W. Cho, J. H. Song, S. Moon, Y. S. Yun, S. J. Kim, Y. W. Lim, D. H. Kim, K. Kang, *Adv. Mater.* **2021**, *33*, 2004902.
[9] I. Huang, Y. Zhang, H. M. Arafa, S. Li, A. Vazquez-Guardado, W. Ouyang, F. Liu, S. Madhvapathy, J. W. Song, A. Tzavelis, J. Trueb, Y. Choi, W. J. Jeang, V. Forsberg, E. Higbee-Dempsey, N. Ghoreishi-Haack, I. Stepien, K. Bailey, S. Han, Z. J. Zhang, C. Good, Y. Huang, A. J. Bandodkar, J. A. Rogers, *Energy Environ. Sci.* **2022**, *15*, 4095.
[10] V. C. Shruti, G. Kutralam-Muniasamy, *Sci. Total Environ.* **2019**, *697*, 134139.
[11] M. Shen, B. Song, G. Zeng, Y. Zhang, W. Huang, X. Wen, W. Tang, *Environ. Pollut.* **2020**, *263*, 114469.

[12] C. J. Bettinger, *Trends Biotechnol.* **2015**, *33*, 575.
[13] C. Steiger, A. Abramson, P. Nadeau, A. P. Chandrakasan, R. Langer, G. Traverso, *Nat. Rev. Mater.* **2019**, *4*, 83.
[14] S. R. McGreevy, C. D. D. Rupprecht, D. Niles, A. Wiek, M. Carolan, G. Kallis, K. Kantamaturapoj, A. Mangnus, P. Jehlička, O. Taherzadeh, M. Sahakian, I. Chabay, A. Colby, J. L. Vivero-Pol, R. Chaudhuri, M. Spiegelberg, M. Kobayashi, B. Balázs, K. Tsuchiya, C. Nicholls, K. Tanaka, J. Vervoort, M. Akitsu, H. Mallee, K. Ota, R. Shinkai, A. Khadse, N. Tamura, K. Abe, M. Altieri, et al., *Nat. Sustain.* **2022**, *5*, 1011.
[15] N. Alexandratos, J. Bruinsma, ESA Working paper No. 12-03 Agricultural and Food Policy **2012**.
[16] R. Gebbers, A. I. Viacheslav, *Science* **2010**, *327*, 828.
[17] J. A. Khan, H. K. Qureshi, A. Iqbal, C. Lacatus, *Comput. Electr. Eng.* **2015**, *41*, 159.
[18] A. S. Sharova, F. Melloni, G. Lanzani, C. J. Bettinger, M. Caironi, *Adv. Mater. Technol.* **2020**, *6*, 2000757.
[19] W. Xu, H. Yang, W. Zeng, T. Houghton, X. Wang, R. Murthy, H. Kim, Y. Lin, M. Mignolet, H. Duan, H. Yu, M. Slepian, H. Jiang, *Adv. Mater. Technol.* **2017**, *2*, 1700181.
[20] Y. Wu, D. Ye, Y. Shan, S. He, Z. Su, J. Liang, J. Zheng, Z. Yang, H. Yang, W. Xu, H. Jiang, *Adv. Mater. Technol.* **2020**, *5*, 2000100.
[21] D. Floreano, B. Kwak, M. Pankhurst, J. Shintake, M. Caironi, V. F. Annese, Q. Qi, J. Rossiter, R. M. Boom, *Nat. Rev. Mater.* **2024**, 1.
[22] P. Cataldi, L. Lamanna, C. Bertei, F. Arena, P. Rossi, M. Liu, F. Di Fonzo, D. G. Papageorgiou, A. Luzio, M. Caironi, *Adv. Funct. Mater.* **2022**, *32*, 2113417.
[23] A. S. Sharova, F. Modena, A. Luzio, F. Melloni, P. Cataldi, F. Viola, L. Lamanna, N. F. Zorn, M. Sassi, C. Ronchi, J. Zaumseil, L. Beverina, M. R. Antognazza, M. Caironi, *Nanoscale* **2023**, *15*, 10808.
[24] A. S. Sharova, M. Caironi, *Adv. Mater.* **2021**, *33*, 2103183.
[25] V. F. Annese, B. Kwak, G. Coco, V. Galli, I. K. Ilic, P. Cataldi, D. Floreano, M. Caironi, *Adv. Sens. Res.* **2023**, *2*, 2300092.
[26] V. F. Annese, V. Galli, G. Coco, M. Caironi, in *Proceedings –2023 9th International Workshop on Advances in Sensors and Interfaces, IWASI 2023*, Institute Of Electrical And Electronics Engineers Inc., **2023**, pp. 236–240.
[27] V. F. Annese, G. Coco, V. Galli, P. Cataldi, M. Caironi, in *2023 IEEE International Conference on Flexible and Printable Sensors and Systems (FLEPS)*, Institute Of Electrical And Electronics Engineers (IEEE), **2023**, pp. 1–4.
[28] I. K. Ilic, L. Lamanna, D. Cortecchia, P. Cataldi, A. Luzio, M. Caironi, *ACS Sens.* **2022**, *7*, 2995.
[29] V. F. Annese, P. Cataldi, V. Galli, G. Coco, J. P. V. Damasceno, A. Keller, Y. Kumaresan, P. Rossi, I. K. Ilic, B. Kwak, L. T. Kubota, A. Athanassiou, J. Rossiter, D. Floreano, M. Caironi, *Adv. Sens. Res.* **2023**, *3*, 2300150.
[30] A. Keller, Q. Qi, Y. Kumaresan, A. T. Conn, J. Rossiter, in *2023 IEEE International Conference on Soft Robotics (RoboSoft)*, IEEE, Singapore, Singapore, April **2023**.
[31] J. Shintake, H. Sonar, E. Piskarev, J. Paik, D. Floreano, in *2017 IEEE/RSJ International Conference on Intelligent Robots and Systems (IROS)*, IEEE, Vancouver, BC, Canada, September **2017**.
[32] Q. Qi, A. Keller, L. Tan, Y. Kumaresan, J. Rossiter, *Mater. Des.* **2023**, *235*, 112339.
[33] C. Gao, C. Bai, J. Gao, Y. Xiao, Y. Han, A. Shaista, Y. Zhao, L. Qu, *J. Mater. Chem. A* **2020**, *8*, 4055.
[34] X. Wang, W. Xu, P. Chatterjee, C. Lv, J. Popovich, Z. Song, L. Dai, M. Y. S. Kalani, S. E. Haydel, H. Jiang, *Adv. Mater. Technol.* **2016**, *1*, 1600059.
[35] L. Lamanna, G. Pace, I. K. Ilic, P. Cataldi, F. Viola, M. Friuli, V. Galli, C. Demitri, M. Caironi, *Nano Energy* **2023**, *108*, 108168.
[36] K. Chen, L. Yan, Y. Sheng, Y. Ma, L. Qu, Y. Zhao, *ACS Nano* **2022**, *16*, 15261.
[37] I. Jeerapan, B. Ciui, I. Martin, C. Cristea, R. Sandulescu, J. Wang, *J. Mater. Chem. B* **2018**, *6*, 3571.
[38] H.-Y. Chen, A. Keller, A. T. Conn, J. Rossiter, in *2023 IEEE International Conference on Soft Robotics (RoboSoft)*, IEEE, Singapore, Singapore, April **2023**, p. 1–6.
[39] L. Lamanna, P. Cataldi, M. Friuli, C. Demitri, M. Caironi, *Adv. Mater. Technol.* **2022**, *8*, 2200731.
[40] I. K. Ilic, V. Galli, L. Lamanna, P. Cataldi, L. Pasquale, V. F. Annese, A. Athanassiou, M. Caironi, *Adv. Mater.* **2023**, *35*, 2211400.
[41] V. Galli, G. Coco, V. F. Annese, M. Caironi, in *2023 IEEE Conference on AgriFood Electronics (CAFE)*, IEEE, Torino, Italy, September **2023**.
[42] V. F. Annese, V. Galli, G. Coco, M. Caironi, *IEEE Trans. AgriFood Electron.* **2024**, p. 1.
[43] J. V. Formica, W. Regelsont, *Food Chem. Toxicol.* **1995**, *35*, 1061.
[44] D. Turck, J. L. Bresson, B. Burlingame, T. Dean, S. Fairweather-Tait, M. Heinonen, K. I. Hirsch-Ernst, I. Mangelsdorf, H. J. McArdle, A. Naska, G. Nowicka, K. Pentieva, Y. Sanz, A. Siani, A. Sjödin, M. Stern, D. Tomé, H. Van Loveren, M. Vinceti, P. Willatts, C. Lamberg-Allardt, H. Przyrembel, I. Tetens, C. Dumas, L. Fabiani, A. C. Forss, S. Ioannidou, M. Neuhäuser-Berthold, *EFSA J.* **2017**, *15*, 04919.
[45] F. Aguilar, R. Crebelli, B. Dusemund, P. Galtier, J. Gilbert, D. M. Gott, U. Gundert-Remy, J. König, C. Lambré, J.-C. Leblanc, A. Mortensen, P. Mosesso, D. Parent-Massin, I. M. C. M. Rietjens, I. Stankovic, P. Tobback, I. Waalkens-Berendsen, R. A. Woutersen, M. Wright, *EFSA J.* **2012**, *10*, 2592.
[46] F. Aguilar, R. Crebelli, A. Di Domenico, B. Dusemund, M. J. Frutos, P. Galtier, D. Gott, U. Gundert-Remy, C. Lambré, J.-C. Leblanc, O. R. Lindtner, P. Moldeus, A. Mortensen, P. Mosesso, A. Oskarsson, D. Parent-Massin, I. Stankovic, I. Waalkens-Berendsen, R. A. Woutersen, M. Wright, M. Younes, *EFSA J.* **2016**, *14*, 4362.
[47] M. Younes, P. Aggett, F. Aguilar, R. Crebelli, A. Di Domenico, B. Dusemund, M. Filipič, M. Jose Frutos, P. Galtier, D. Gott, U. Gundert-Remy, G. Georg Kuhnle, C. Lambré, J. C. Leblanc, I. T. Lillegaard, P. Moldeus, A. Mortensen, A. Oskarsson, I. Stankovic, P. Tobback, I. Waalkens-Berendsen, M. Wright, A. Tard, S. Tasiopoulou, R. A. Woutersen, *EFSA J.* **2018**, *16*, 05047.
[48] M. Younes, G. Aquilina, L. Castle, K. H. Engel, P. Fowler, P. Fürst, R. Gürtler, U. Gundert-Remy, T. Husøy, W. Mennes, P. Moldeus, A. Oskarsson, R. Shah, I. Waalkens-Berendsen, D. Wölfle, P. Boon, R. Crebelli, A. Di Domenico, M. Filipič, A. Mortensen, H. Van Loveren, R. Woutersen, A. Giarola, F. Lodi, F. Riolo, M. J. Frutos Fernandez, *EFSA J.* **2019**, *17*, 05868.
[49] F. Aguilar, H. Autrup, S. Barlow, L. Castle, R. Crebelli, W. Dekant, K.-H. Engel, N. Gontard, D. Gott, S. Grilli, R. Gürtler, J. C. Larsen, C. Leclercq, J,-C. Leblanc, F. X. Malcata, W. Mennes, M. R. Milana, I. Pratt, I. Rietjens, P. Tobback, F. Toldrá, *EFSA J.* **2007**, *615*, 1.
[50] H. Wang, Z. Chen, Z. Ji, P. Wang, J. Wang, W. Ling, Y. Huang, *Mater. Today Energy* **2021**, *19*, 100577.
[51] D. Kumar, Z. Khan, U. Ail, J. Phopase, M. Berggren, V. Gueskine, X. Crispin, *Adv. Energy Sustainability Res.* **2022**, *3*, 2200073.
[52] F. Fratini, G. Cilia, B. Turchi, A. Felicioli, *Asian Pac. J. Trop. Med.* **2016**, *9*, 839.
[53] R. Arbaud, M. Najafi, J. M. Gandarias, M. Lorenzini, U. C. Paul, A. Zych, A. Athanassiou, P. Cataldi, A. Ajoudani, *Adv. Mater. Technol.* **2024**, *9*, 2301265.
[54] A. Chamas, H. Moon, J. Zheng, Y. Qiu, T. Tabassum, J. H. Jang, M. Abu-Omar, S. L. Scott, S. Suh, *ACS Sustainable Chem. Eng.* **2020**, *8*, 3494.
[55] K. Miyaji, C. Zhou, A. Maeda, K. Kobayashi, R. Kusumi, M. Wada, *Polym. Degrad. Stab.* **2023**, *215*, 110423.
[56] M. A. Acquavia, J. J. Benítez, G. Bianco, M. A. Crescenzi, J. Hierrezuelo, M. Grifé-Ruiz, D. Romero, S. Guzmán-Puyol, J. A. Heredia-Guerrero, *Food Chem.* **2023**, *429*, 136906.
[57] G. Spallanzani, M. Najafi, M. Zahid, E. L. Papadopoulou, L. Ceseracciu, M. Catalano, A. Athanassiou, P. Cataldi, A. Zych, *Adv. Sustainable Syst.* **2023**, *7*, 2300220.
[58] R. Pantani, A. Sorrentino, *Polym. Degrad. Stab.* **2013**, *98*, 1089.